

## STOCHASTIC APPROACH TO HOPPING TRANSPORT IN DISORDERED ORGANIC MATERIALS

E. V. Emelianova, G. J. Adriaenssens\*

Semiconductor Physics Laboratory, University of Leuven, Celestijnenlaan 200D, B-3001 Leuven, Belgium

At variance with inorganic amorphous semiconductors, all electronic states in disordered organics are localized and electrical conduction can proceed by carrier hopping within the manifold of those states that are, therefore, often referred to as hopping sites. One of the most common approach to the description of charge transport in such systems is the variable-range hopping theory. While the general principles of this theory have been known and accepted for years, many important aspects and applications of this theory have only been examined more recently. In this survey we discuss a number of facets of hopping in disordered organic materials that have not received much attention in the past. Following a general outline of the calculation of the equilibrium mobility it is shown how the concept of an effective transport energy effectively reduces the description of hopping a much simpler problem of trap-controlled band transport. The influence of high carrier densities and of defect centers on the carrier mobility as well as the special case of space charge limited currents are discussed in detail. In subsequent sections, the effect of doping on the density-of-states distribution and on transport characteristics are considered. The effect of polaron formation and deep trapping on the activation energy of the carrier mobility in disordered organic materials are the subject of our final section.

(Received October 25, 2004; accepted November 29, 2004)

*Keywords:* Organic materials, Hopping transport, Stochastic approach

### 1. Equilibrium hopping mobility in a positionally random and energetically disordered hopping system

#### A general method

Charge carrier transport in organic materials as well as in non-crystalline solids is known to be governed by positional and energy disorder. The presence of positional disorder inevitably gives rise to the energy disorder via dependence of the potential energy of interaction upon the distance between interacting particles [1,2]. Due to disorder effects, carriers are almost permanently localised and the only feasible mode of charge transport is carrier jumps directly between localized states. The mechanism is often referred to as hopping [3]. Most hopping models are based on the Miller-Abrahams [4] expression for the probability  $\nu$  of a tunnelling jump between a starting state  $E_{st}$  to a vacant target site of the energy  $E_t$ .

$$\nu(r, E_{st}, E_t) = \nu_0 \exp[-u(r, E_{st}, E_t)], \quad u(r, E_{st}, E_t) = 2\gamma + \frac{\eta(E_t - E_{st})}{kT}, \quad (1)$$

where  $\gamma$  is the inverse localization radius of the electronic wavefunction,  $\nu_0$  the attempt-to-jump frequency,  $T$  the temperature,  $k$  the Boltzmann constant, and  $\eta$  the unity step-function.

---

\* Corresponding author: guy.adri@fys.kuleuven.ac.be

Since the hopping rate exponentially decreases with increasing energy difference and with increasing distance between localized states, most carriers will jump to target sites characterized by minimum values of the hopping parameter  $u$ . Hereafter, such target sites will be referred to as nearest hopping neighbours. Under these conditions, the average jump rate for a carrier localized in a site of the energy  $E_{st}$  can be found by the use of the Poisson distribution [5,6]. For a starting site of energy  $E_{st}$ , the average number,  $n_0(E_{st}, u)$ , of hopping neighbours, whose hopping parameter is not larger than  $u$ , is given by,

$$\begin{aligned} n_0(E_{st}, u) &= 4\pi \int_0^{u/2\gamma} dr r^2 \int_{-\infty}^{E_{st}+kT(u-2\gamma)} dE_t g(E_t) = \\ &= \frac{4\pi}{3} \left( \frac{u}{2\gamma} \right)^3 \left[ \int_{-\infty}^{E_{st}} dE_t g(E_t) + \int_{E_{st}}^{E_{st}+kTu} dE_t g(E_t) \left( 1 - \frac{E_t - E_{st}}{kTu} \right)^3 \right], \end{aligned} \quad (2)$$

where  $g(E)$  is the density-of-states (DOS) distribution. The first term in the right-hand side of Eq. (2) gives the number of target states that are deeper than the starting site and the second one describes the number of shallower states. The former is important as far as downward carrier jumps are concerned while the latter governs the rate of upward jumps. Since the probability density,  $w_0(E_{st}, u)$ , that a nearest hopping neighbour has the hopping parameter  $u$  is determined by the Poisson distribution  $w_0(E_{st}, u) = \exp[-n_0(E_{st}, u)] \frac{\partial n_0(E_{st}, u)}{\partial u}$ , the average hopping parameter,  $\langle u \rangle_0(E_{st})$ , for carrier jumps from a starting site  $E_{st}$  can be written as

$$\langle u \rangle_0(E_{st}) = \int_0^{\infty} du u \exp[-n_0(E_{st}, u)] \frac{\partial n_0(E_{st}, u)}{\partial u} = \int_0^{\infty} du \exp[-n_0(E_{st}, u)] \quad (3)$$

The average squared jump distance,  $\langle r^2 \rangle_0(E_{st})$ , can be evaluated as,

$$\begin{aligned} \langle r^2 \rangle_0(E_{st}) &= \frac{4\pi}{n_0(E_{st}, \langle u \rangle_0)} \int_0^{\langle u \rangle_0/2\gamma} dr r^4 \int_{-\infty}^{E_{st}+kT(\langle u \rangle_0-2\gamma)} dE_t g(E_t) = \\ &= \frac{3}{5} \left( \frac{\langle u \rangle_0}{2\gamma} \right)^2 \left[ \int_{-\infty}^{E_{st}} dE_t g(E_t) + \int_{E_{st}}^{E_{st}+kT\langle u \rangle_0} dE_t g(E_t) \left( 1 - \frac{E_t - E_{st}}{kT\langle u \rangle_0} \right)^5 \right] \\ &\quad \times \left[ \int_{-\infty}^{E_{st}} dE_t g(E_t) + \int_{E_{st}}^{E_{st}+kT\langle u \rangle_0} dE_t g(E_t) \left( 1 - \frac{E_t - E_{st}}{kT\langle u \rangle_0} \right)^3 \right]^{-1}. \end{aligned} \quad (4)$$

Averaging hopping rates over  $E_{st}$  and using the Einstein relation yields the following expression for the equilibrium mobility  $\mu_0$ :

$$\mu_0 = \frac{eV_0}{kT} \int_{-\infty}^{\infty} dE_{st} \exp[-\langle u \rangle_0(E_{st})] \langle r^2 \rangle_0(E_{st}) f(E_{st}) \quad (5)$$

where  $f(E)$  is the normalized energy distribution function of localized carriers. Without dramatic loss of accuracy, the rather complicated Eq. (5) for the average squared jump distance, can be replaced by a simpler estimate  $\langle r^2 \rangle_0(E_{st}) \approx (\langle u \rangle_0/2\gamma)^2$ .

The time-of-flight (TOF) technique is commonly used for the experimental study of charge carrier mobility in both organic and inorganic non-crystalline materials. TOF measurements imply a low carrier density that allows neglecting the possibility of trap filling. Under these conditions one

can use a single-carrier distribution function in Eq. (5). The equilibrium TOF mobility can, therefore, be calculated by the use of the normalized Boltzmann distribution

$$f(E) = \left[ \int_{-\infty}^{\infty} dE g(E) \exp\left(-\frac{E}{kT}\right) \right]^{-1} g(E) \exp\left(-\frac{E}{kT}\right) \text{ as}$$

$$\mu_0 = \frac{eV_0}{kT} \left[ \int_{-\infty}^{\infty} dE_{st} g(E_{st}) \exp\left(-\frac{E_{st}}{kT}\right) \right]^{-1} \times \int_{-\infty}^{\infty} dE_{st} \exp[-\langle u \rangle_0(E_{st})] \langle r^2 \rangle_0(E_{st}) g(E_{st}) \exp\left(-\frac{E_{st}}{kT}\right) \quad (6)$$

The result given by Eq (5) is obtained without accounting the possibility of backward carrier jumps into starting sites. For the dc conductivity it is essential that the downward jumps occur to states *other* than starting ones. In a hopping system, a target site is a localized state that normally has only few hopping neighbours accessible for a next jump and it is quite possible that, after an upward jump, a carrier will return to the initially occupied deeper site. Such a jump contributes to neither dc transport nor energy relaxation.

After an upward jump over the distance  $r$ , a carrier will, most probably, not return to the starting site if there is another hopping neighbour of the target site with a hopping parameter that is smaller than  $2\gamma$  *outside* the sphere of radius  $r$  centred at the starting site. The average number of such neighbours,  $n_b(E_t, r)$ , increases with increasing  $E_t$  and  $r$  as,

$$n_b(E_t, r) = 2\pi \int_0^r dr' r'^2 \int_{\arccos(r'/2r)}^{\pi} d\vartheta \sin \vartheta \int_{-\infty}^{E_t + 2\gamma kT(r-r')} dE' g(E') =$$

$$= \frac{\pi r^3}{12} \left\{ 11 \int_{-\infty}^{E_t} dE' g(E') + \int_{E_t}^{E_t + 2\gamma kT r} dE' g(E') \left[ 8 \left( 1 - \frac{E' - E_t}{2kT\gamma} \right)^3 + 3 \left( 1 - \frac{E' - E_t}{2kT\gamma} \right)^4 \right] \right\} . \quad (7)$$

Since the round-trip carrier jumps do not contribute to transport and relaxation, only those hopping neighbours should be accounted for from which carrier jumps back to initially occupied starting sites are improbable. The average number  $n(E_{st}, u)$  of such hopping neighbours, therefore, can be written for upward jumps as:

$$n(E_{st}, u) = 4\pi \int_{E_s}^{E_{st} + kTu} dE_t g(E_t) \int_0^{(1/2\gamma)[u - (E_t - E_{st})/kT]} dr r^2 \{1 - \exp[-n_b(E_t, r)]\} . \quad (8)$$

The average hopping parameter,  $\langle u \rangle(E_{st})$ , can be calculated by the use of Eq. (3), with the function  $n(E_{st}, u)$  instead of  $n_0(E_{st}, u)$ , and the average square jump distance  $\langle r^2 \rangle(E_{st})$  can be estimated as  $\langle r^2 \rangle(E_{st}) \approx (\langle u \rangle / 2\gamma)^2$  or evaluated from Eq. (4) with the function  $n_0(E_{st}, u)$  substituted by function  $n(E_{st}, u)$ .

### Effective transport energy

The calculation of both the mobility and conductivity can be significantly simplified if the concept of the effective transport energy is employed. This method is based on the notion that, after an energetically upward jump into a hopping site that belongs to the transport level, a carrier will make several downward jumps, which effectively reduces hopping to trap-controlled transport [7]. The occurrence of an effective transport energy was first revealed in Monte-Carlo simulation [8] and was later proven by analytic consideration of charge carrier kinetics in disordered hopping systems [9]. In general, the probability that a jump will be made to some site of the specific energy  $E_t$  depends upon the temperature, the density-of-state distribution, the localization radius, *and* the energy of the starting site. However, if the DOS function is sufficiently steep and if the starting site

is sufficiently deep, the most probable value of the energy  $E_t$  does not depend upon  $E_{st}$ . In other words, practically all carriers, localised in a deep tail of the DOS distribution will sooner or later jump to one of the shallower states whose energies are close to some universal value which is traditionally referred to as the transport energy,  $E_{tr}$ .

In order to obtain an expression for transport energy, one can carry out the replacement  $E_j = E_{st} + kTu$  in Eq. (2), where  $n_0(E_{st}, E_j) = 1$ , i.e. an upward carrier jump from a starting site is possible if there is at least one such hopping neighbour. The transcendental equation for the energy of the most probable upward jumps can be written [7]:

$$\int_{E_{st}}^{E_j} dE_t g(E_t) (E_j - E_t)^3 = \frac{6}{\pi} (\gamma kT)^3 . \quad (9)$$

If the DOS distribution decreases with energy faster than  $|E|^{-4}$  than (i) the value of the integral in the left-hand side of Eq. (9) is practically independent of the lower bound of integration for sufficiently deep starting sites and (ii) a major contribution to the integral comes from states with energies around  $E_j$ . Physically, it means that target sites for thermally assisted upward carrier jumps are located around the energy  $E_j$  independent of the energy of starting sites and, therefore, Eq. (9) reduces to:

$$\int_{-\infty}^{E_j} dE_t g(E_t) (E_j - E_t)^3 = \frac{6}{\pi} (\gamma kT)^3 . \quad (10)$$

Equation (9) for the energy of most probable jumps was derived from Eq. (2) for the average number of hopping neighbours. This equation does not account for the possibility of round-trip jumps between occasionally close hopping sites. This implies a possibility that carrier jumps to the energy  $E_j$  will be mostly followed by backward jumps to initially occupied sites. In order to preclude this possibility and obtain an equation for the genuine transport energy one should use Eq. (8) instead of Eq. (2) for the number of hopping neighbours:

$$4\pi \int_{-\infty}^{E_{tr}} dE_t g(E_t) \int_0^{(E_{tr}-E_t)/2\gamma kT} dr r^2 \left\{ 1 - \exp\left[-n_b(E_t, r)\right] \right\} = 1 , \quad (11)$$

where  $n_b(E_t, r)$  is given by Eq. (7). The energy  $E_{tr}$  is the minimum energy to which carriers must jump in order to contribute to the dc conductivity. This notion implies similarity between the effective transport level in variable-range hopping and the mobility edge in trap-controlled band transport. In general, once the effective transport energy is calculated, the hopping problem is virtually reduced to a much simpler problem of carrier multiple trapping in an energetically disordered system of localized states [10-12].

The difference between temperature dependencies of the effective transport energy and the energy of most probable jumps is illustrated in Fig. 1 for a random hopping system with a Gaussian DOS distribution of the width  $\sigma$ ,

$$g(E) = \frac{N}{\sqrt{2\pi}\sigma} \exp\left(-\frac{E^2}{2\sigma^2}\right) , \quad (12)$$

parametric in the density of hopping sites  $N$ . Solid lines in this figure show the temperature dependencies of the energy of most probable upward jumps calculated from Eq. (10) without accounting for backward jumps. The dashed lines were calculated from Eq. (11). The difference between dashed and solid lines for each DOS is significant and more noticeable at higher temperatures and/or at lower concentrations of localized states.

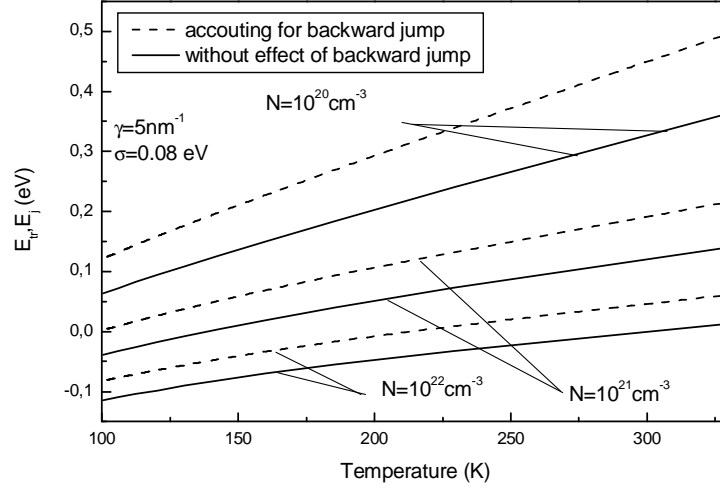


Fig. 1. Temperature dependencies of the effective transport energy and the energy of most probable jumps in a disordered hopping system with a Gaussian DOS distribution, parametric in total density of localized states  $N$ . The data shown by the solid and dashed lines are calculated from eqns. (10) and (11), respectively, for  $\gamma = 5 \text{ nm}^{-1}$ , and  $\sigma = 0.08 \text{ eV}$ .

Averaging rates of carrier jumps to the effective transport level, estimating the average square jump distance as  $\langle r^2 \rangle = \left[ \int_{-\infty}^{E_{tr}} dE g(E) \right]^{-2/3}$ , and using the Einstein relation yields the following expression for the equilibrium mobility:

$$\mu = \frac{eV_0}{kT} \left[ \int_{-\infty}^{E_{tr}} dE g(E) \right]^{-2/3} \int_{-\infty}^{E_{tr}} dE_{st} f(E_{st}) \exp\left(-\frac{E_{tr} - E_{st}}{kT}\right). \quad (13)$$

For the single-particle Boltzmann distribution function this expression yields

$$\mu_b = \frac{eV_0}{kT} \left[ \int_{-\infty}^{\infty} dE g(E) \exp\left(-\frac{E}{kT}\right) \right]^{-1} \left[ \int_{-\infty}^{E_{tr}} dE g(E) \right]^{1/3} \exp\left(-\frac{E_{tr}}{kT}\right), \quad (14)$$

where  $E_{tr}$  can be calculated either from Eq. (11) or, as a rougher approximation, from Eq. (10) that disregards the effect of round-trip carrier jumps.

The expression for the equilibrium carrier mobility derived on the basis of the effective transport energy concept and given by Eq. (13) is simpler and more feasible for applications than the use of Eq. (5). Temperature dependences of the mobility, calculated from Eqs. (5), (10), (11), and (13) for a Gaussian DOS distribution of the width  $\sigma = 0.08 \text{ eV}$  are shown in Fig. 2 for different values of the total density of localized states  $N$ . All the curves feature almost perfect straight lines if plotted as  $\log \mu$  vs  $1/T^2$ . Although absolute values of the mobility strongly depend upon  $N$ , the slope increases by a few percent when the density of hopping sites decreases by three orders of magnitude. The solid and dashed lines show the equilibrium mobility calculated without consideration of the round-trip hopping while the dotted curves show the effect of backward jumps. Taking into account the possibility of backward jumps leads to a significant decrease in the value of the carrier equilibrium mobility by more than two orders of magnitude especially at lower temperatures and/or lower densities of localized states.

### The effect of high carrier density on the equilibrium hopping mobility

Electronic applications of disordered semiconductors imply high densities of the injection current and/or high doping levels in these materials. Realistic operating conditions for organic light emitting diodes (OLEDs) in active matrix colour displays are at some 500 to 1000 Cd/m<sup>2</sup> peak. In monochrome passive matrix displays, the peak brightness can be several 1000 Cd/m<sup>2</sup>. For yellow-orange, an efficiency of 10 Cd/A is typical, be it not at the highest brightness. The maximum current density in monochrome passive matrix displays is therefore of the order of several 10 mA/cm<sup>2</sup> to 100 mA/cm<sup>2</sup>. For active matrix colour displays, the largest current densities will be found for blue due to the poor eye sensitivity, and are of the order of hundred mA/cm<sup>2</sup>. Further assuming a mobility of the order of 10<sup>-7</sup> to 10<sup>-6</sup> cm<sup>2</sup>V<sup>-1</sup>s<sup>-1</sup>, a layer thickness of 100 nm, and a voltage drop over the organic material, not including the contacts, of 5 V to 10 V depending on the colour, and a current density of several 10 to 100 mA/cm<sup>2</sup>, the maximum carrier density in OLEDs can be as high as 10<sup>17</sup> cm<sup>-3</sup> to a few times 10<sup>18</sup> cm<sup>-3</sup>.

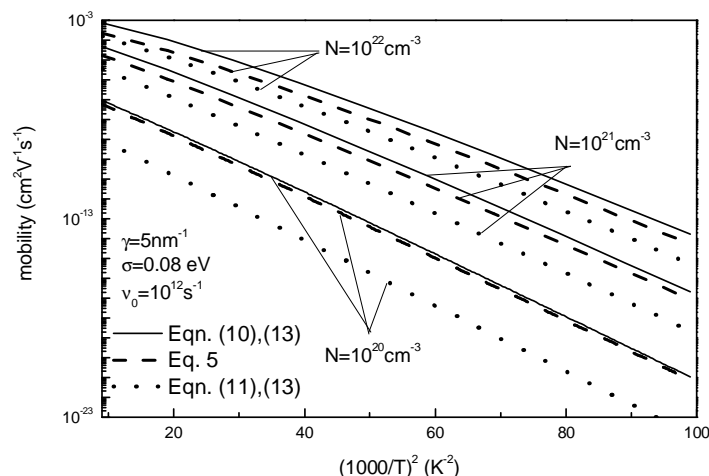


Fig. 2. Temperature dependence of the equilibrium drift mobility in a disordered hopping system with a Gaussian DOS distribution of localized states for different values of the total density of localized states  $N$ . Solid, dashed and dotted lines are calculated from eqns. (10) and (13), (5), (11) and (13), respectively, for  $\gamma = 5 \text{ nm}^{-1}$ ,  $\sigma = 0.08 \text{ eV}$ ,  $\nu_0 = 10^{12} \text{ s}^{-1}$ .

For organic thin film transistors, typical mobilities are much higher. For polymers, reported mobilities range between a few 10<sup>-3</sup> to several 10<sup>-1</sup> cm<sup>2</sup>V<sup>-1</sup>s<sup>-1</sup>, while for polycrystalline materials like pentacene they range from a few 10<sup>-1</sup> to a few cm<sup>2</sup>V<sup>-1</sup>s<sup>-1</sup>. The typical surface carrier density accumulated under the gate insulator is then of the order of 10<sup>12</sup> cm<sup>-2</sup> to 10<sup>13</sup> cm<sup>-2</sup>. The accumulated charge is localized in a sheet not thicker than a few nanometers. The carrier density in that sheet therefore turns out to be of 10<sup>18</sup> cm<sup>-3</sup> to 10<sup>19</sup> cm<sup>-3</sup>.

Since the carrier density in a doped polymer can be comparable with the density of localized states, hopping sites in the deep tail of the DOS distribution can be fully filled by carriers. The filling affects energy distributions of both localized carriers and vacant hopping sites. Therefore, the field and temperature dependencies of the conductivity must be sensitive to the density of charge carriers. The normalized thermal equilibrium energy distribution of localized carriers is given by a product of the Fermi-Dirac function and the DOS distribution as

$$f(E) = \frac{g(E)}{1 + \exp[(E - E_F)/kT]} \left\{ \int_{-\infty}^{\infty} \frac{dE' g(E')}{1 + \exp[(E' - E_F)/kT]} \right\}^{-1} \quad (15)$$

where the Fermi energy  $E_F$  is determined by the total carrier density  $p$  via the following transcendental equation:

$$p = \int_{-\infty}^{\infty} \frac{dE g(E)}{1 + \exp[(E - E_F)/kT]} \quad (16)$$

Concomitantly, the density of vacant hopping sites,  $g_v(E)$ , should be equal to the difference of the DOS function and the density of occupied sites:

$$g_v(E) = g(E) - pf(E) = \frac{g(E)}{1 + \exp[-(E - E_F)/kT]} \quad (17)$$

Well above the Fermi level, i.e. for  $E - E_F \gg kT$ , the density of vacant hopping sites is practically equal to the total density of states. Therefore, if the effective transport energy, obtained while taking the filling of localized states into account, satisfies the condition  $E_{tr} - E_F \gg kT$  the mobility can still be calculated from Eq. (13) with the carrier distribution function given by Eq. (15). The temperature dependence of the mobility calculated for a Gaussian DOS distribution is shown in Fig. 3 parametric in the carrier density  $p$ . At higher temperatures, the conductivity is due to jumps of carriers localized above the Fermi level and, concomitantly, the mobility weakly depends upon the carrier density. At lower temperatures, carrier hopping from the Fermi level takes over and the mobility reveals an Arrhenius-like behavior with the activation energy decreasing with increasing carrier density as shown in the inset to Fig. 3.

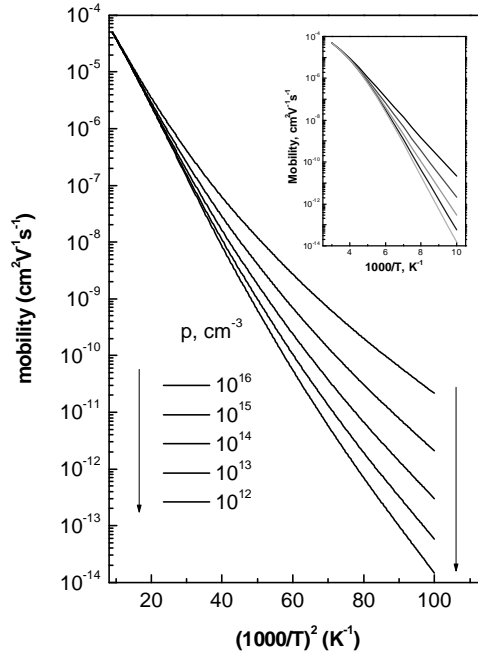


Fig. 3. Temperature dependence of the equilibrium mobility in a disordered hopping system with a Gaussian DOS distribution parametric in the carrier density for the following set of material parameters:  $\gamma = 5 \text{ nm}^{-1}$ ,  $N = 10^{21} \text{ cm}^{-3}$ ,  $\sigma = 0.08 \text{ eV}$ ,  $\nu_0 = 10^{12} \text{ s}^{-1}$ . The inset shows the Arrhenius plot for the same set of data.

The concept of the effective transport energy is applicable if the effective transport level is located well above the Fermi level. However, this condition may not be fulfilled if the temperature is low and/or the carrier density is high. Under such conditions, the effect of filling requires the use of a more sophisticated model based on the averaging of the hopping parameter. In particular, the carrier mobility can be calculated from Eqs. (13) and (14) in which the function  $g(E)$  is replaced by  $g_v(E)$  and the carrier distribution function is given by Eq. (15); transport energy needed for Eq. (18) can be obtained from Eq. (10) with function  $g(E)$  substituted by  $g_v(E)$ .

$$\mu = \frac{e v_0}{k T p} \left[ \int_{-\infty}^{E_{tr}} dE g(E) \right]^{-2/3} \int_{-\infty}^{E_{tr}} \frac{dE g(E)}{1 + \exp[(E - E_F)/kT]} \exp\left(\frac{E - E_{tr}}{kT}\right). \quad (18)$$

It is worth noting that, in materials with a Gaussian DOS distribution, the position of the Fermi level is not always essential for the charge transport characteristics because, under realistic conditions, the majority of charge carriers can occupy weakly filled states above the Fermi level [13]. Therefore, the equilibrium mobility can be affected by filling of deep localized states only at sufficiently high carrier densities.

The dependences of the mobility calculated from Eq. (18) upon the carrier density are shown in Fig. 4 for different initial Gaussian DOS (Eq. (12)) widths. Although the mobility remains practically constant at low carrier densities it strongly increases at higher carrier concentrations. These results prove that the time-of-flight (TOF) mobility in a given material can be much smaller than the mobility estimated from, for example, IV characteristics of the space charge limited currents measured in the same material under the conditions of strong charge injection. It is worth noting that the curves shown in Fig. 4 were calculated under the assumption that the DOS itself is fixed and not affected by the increasing carrier density. However, doping can significantly change the DOS distribution and this effect will be considered in the following section.

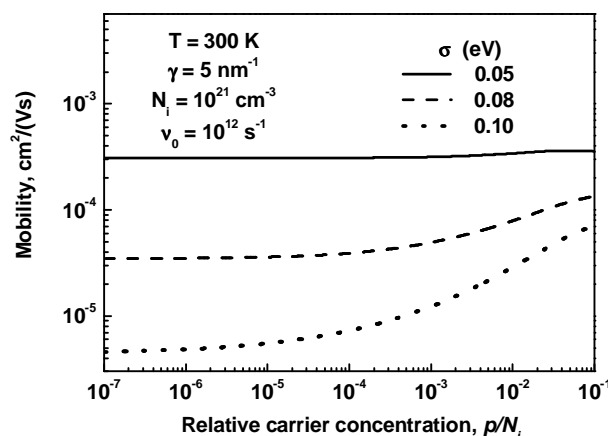


Fig. 4. Dependence of the equilibrium mobility on the charge carrier concentration in a hopping system with a fixed width of a Gaussian DOS distribution.

The dependences calculated from Eq. (18) are shown by solid lines in Fig. 5 together with experimental data obtained on PHT films of 54%, 70%, and 81% of regioregularity [14].

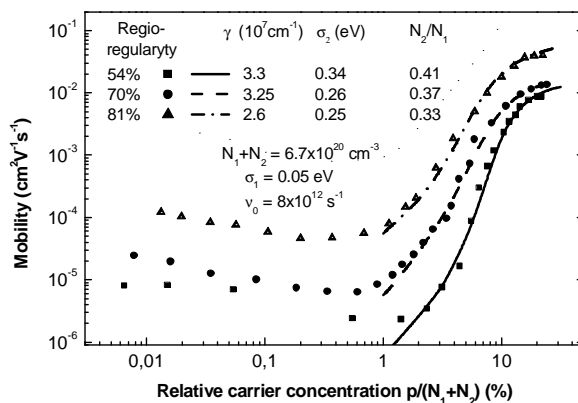


Fig. 5. Dependence of the equilibrium hopping mobility upon the dopant concentration in a disordered organic semiconductor. Experimental points are taken from Ref. [14].

In these materials, interchain carrier jumps along the stacking direction has been suggested as a predominant conductivity mode. In terms of hopping transport this implies the occurrence of a double-peak Gaussian distribution, [6]

$$g(E) = \frac{N_1}{\sqrt{2\pi}\sigma_1} \exp\left(-\frac{E^2}{2\sigma_1^2}\right) + \frac{N_2}{\sqrt{2\pi}\sigma_2} \exp\left(-\frac{E^2}{2\sigma_2^2}\right), \quad (19)$$

in which the first narrow peak describes ordered regions and the second one corresponds to amorphous phase, i.e.  $\sigma_2 \gg \sigma_1$ . For materials with relatively high degrees of regioregularity one should also assume that  $N_1 > N_2$ . At large relative densities of charge carriers, i.e., at total carrier density  $p > 0.01(N_1 + N_2)$ , the agreement between measured and calculated data in Fig. 4 is very gratifying. It is also remarkable that the experimental results for systems with different degrees of regioregularity can be fitted under the premise of an undistorted Gaussian-shaped DOS distribution. However, one has to assume unusually large widths of the DOS distribution in the disordered phase,  $\sigma_2 = 0.25 \dots 0.34$  eV although the parent conjugated polymer features a low degree of disorder. This indicates that the DOS width must strongly increase with increasing density of charge carriers such that variations of the energy levels of the hole transporting moieties, caused by different degrees of regioregularity, are smeared out.

These results imply a very strong effect of the Coulomb interactions on the energy disorder in doped organic semiconductors. It was already recognized that the dipole-dipole interaction between randomly located and oriented dipoles is one of the major causes of energy disorder in organic materials [15]. Increasing regioregularity can suppress this type of disorder and, concomitantly, improve the mobility at low carrier concentrations as one can see from Fig. 5. However, a higher density of randomly distributed charge carriers generates a random Coulomb potential distribution, which effectively broadens the DOS distribution. This effect, discussed more fully in a later section, occurs together with the filling of deep traps. At relatively low carrier densities the Coulomb DOS broadening dominates while most carriers still occupy sites above the Fermi level. Under these conditions, the mobility decreases with increasing carrier concentration. At higher carrier densities the Coulomb-induced DOS broadening almost saturates while the energy distribution of localized carriers becomes shallower which leads to a higher average jump rate and steeply increasing mobility with further increase of carrier density.

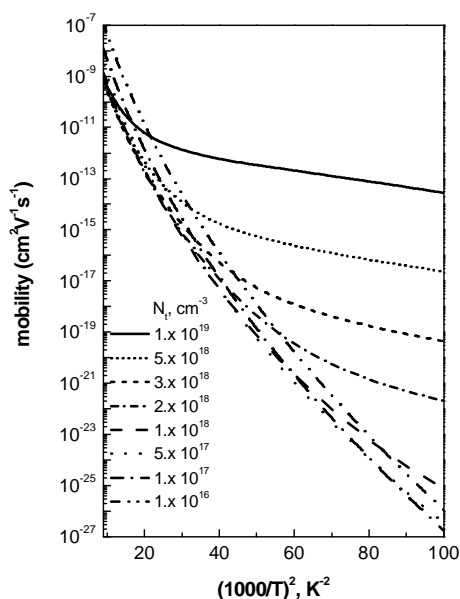


Fig. 6. The effect of deep traps on the temperature dependence of the equilibrium mobility in a disordered hopping system with a Gaussian DOS distribution. The following set of material parameters was used for the calculation:  $\gamma = 5 \text{ nm}^{-1}$ ,  $\nu_0 = 10^{12} \text{ s}^{-1}$ ,  $N_i = 10^{21} \text{ cm}^{-3}$ ,  $\sigma_1 = 0.08 \text{ eV}$ ,  $\sigma_2 = 0.03 \text{ eV}$ ,  $E_t = 0.6 \text{ eV}$ .

### Trap-controlled variable-range hopping

In addition to the intrinsic DOS distribution, disordered organic semiconductors often have deeper localized states originating either from impurities or from chemical and structural defects. Those states are normally located well below the intrinsic DOS distribution and, therefore, they are often referred to as deep traps. Although the total density of traps is much smaller than the density of intrinsic hopping sites, they can, especially at lower temperatures, change the effective transport energy. In addition, these traps can strongly affect charge transport characteristics because, under equilibrium conditions, most carriers will occupy those deep states. In order to calculate the trap-controlled variable-range hopping mobility, one may use either the method based on averaging the hopping parameter, or the effective transport energy concept with a DOS distribution that incorporates both the intrinsic DOS and a distribution of deep traps as

$$g(E) = \frac{N_i}{\sqrt{2\pi}\sigma_i} \exp\left(-\frac{E^2}{2\sigma_i^2}\right) + \frac{N_t}{\sqrt{2\pi}\sigma_t} \exp\left[-\frac{(E - E_t)^2}{2\sigma_t^2}\right], \quad (20)$$

where  $N_i$  and  $N_t$  are the total densities of intrinsic sites and traps, respectively,  $\sigma_i$  and  $\sigma_t$  the Gaussian variations of the intrinsic site and trap distributions, respectively, and  $E_t$  is the energy of the trap DOS maximum. Temperature dependences of the equilibrium trap-controlled TOF mobility are illustrated in Fig. 6 for different trap concentrations. At higher temperatures, practically all carriers occupy intrinsic sites and the occurrence of traps does not change the linear  $\log \mu$  vs  $1/T^2$  dependence that is typical for trap-free disordered organic materials. At lower temperatures, the carrier distribution is pinned at the trap peak. Although the effective transport energy is less sensitive to changing temperature than the equilibrium carrier distribution, it is also affected by the traps especially at high trap densities as one can see from the Fig. 7. In fact, traps can serve as an effective hopping transport band at low  $T$  and high  $N_t$ . Pinning the carrier distribution at an almost fixed energy such as  $E_t$  and steeper temperature dependence of the effective transport energy lead to a weaker  $T$ -dependence of  $\mu$  at lower temperatures.

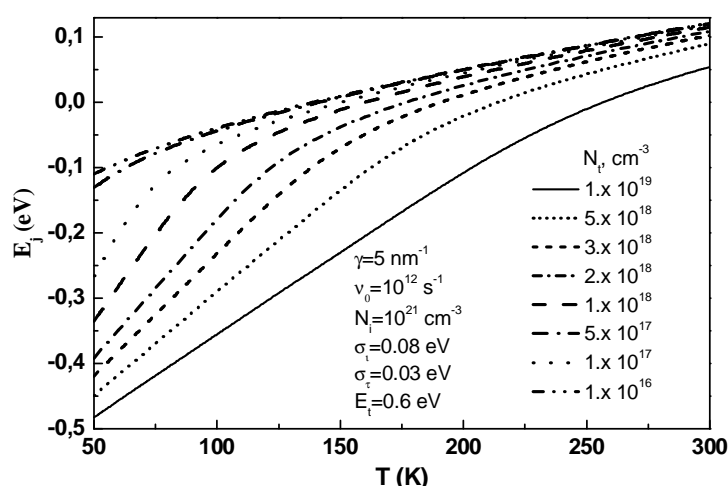


Fig. 7. The temperature dependence of the energy of most probable jumps for the same values of  $N_t$  that used in Fig. 5, for the following set of material parameters:  $\gamma = 5 \text{ nm}^{-1}$ ,  $v_0 = 10^{12} \text{ s}^{-1}$ ,  $N_i = 10^{21} \text{ cm}^{-3}$ ,  $\sigma_i = 0.08 \text{ eV}$ ,  $\sigma_t = 0.03 \text{ eV}$ ,  $E_t = 0.6 \text{ eV}$ .

## 2. Variable range hopping in doped organic materials

As shown in the preceding sections, charge carrier hopping within a positionally random and energetically disordered system of localized states is an adequate model for the description of charge

transport in disordered organic semiconductors. In a non-crystalline material, the energy disorder is mostly due to Van der Waals and dipole-dipole interactions within a positionally and orientationally random system of molecules [16]. Doping of such a system creates, in addition, a random distribution of dopant ions that will Coulombically interact with carriers localized in intrinsic hopping sites. This interaction further increases the energy disorder. This effect is especially important in view of a small value of the dielectric constant and, concomitantly, long range of the Coulomb interaction typical for molecular semiconductors. Increasing energy disorder with increasing dopant concentration will lead to broadening of the effective density-of-states distribution.

Doping of a disordered organic semiconductor by charged moieties has two counteracting effects. On the one hand, it increases the concentration of charge carriers and lifts up the Fermi level [17,18] but, on the other hand, it increases energetic disorder. While the former effect facilitates conductivity, the latter strongly suppresses the carrier hopping rate and, therefore, the mobility. The latter effect can dominate at some dopant concentrations such that doping appears to be even counterproductive as far as the carrier mobility is concerned. [17,14].

Upon doping by ionized moieties charge neutrality must be maintained. There are two ways to accomplish this. One is electrochemical doping. If the ionization (or reduction) potential of the electrolyte electrode more or less matches the highest occupied molecular orbital (HOMO) of the organic semiconductor mobile majority carriers can be injected provided that the electrolyte supplies appropriate counterions that can diffuse into the semiconductor. An example is the work of Jiang *et al.* [14] who injected holes from a solution of 0.1 M tetraethylammonium perchlorate into a film of poly-hexylthiophene. Charge injection was compensated by concomitant doping with (permanent) perchlorate anions. The alternative method is doping by a neutral entity whose electron affinity is large enough (or its ionization energy is small enough) to allow for charge transfer from the semiconductor to the dopant [19]. Dictated by the redox potential of donor-acceptor systems and, concomitantly, the dissociation enthalpy, complete charge transfer and creation of free carriers in the dark is in practice never possible, i.e. charge full transfer is an endothermic and reversible process.

Both modes of doping resemble the situation Onsager had in mind when he developed his 1934 and 1938 treatments of ionic and radiation-induced conductivity [20,21]. In both cases excess mobile majority carriers and immobile counter charges (ions) are generated that roughen the energy landscape in which the carriers migrate but in the ‘neutral’ doping case also charge redistribution can and does occur. The majority of charge carriers will actually form metastable geminate pairs whose dissociation is facilitated by the ambient phonon bath and external electric field. Therefore, the average hopping rate is controlled by the carrier release from the Coulomb traps, i.e. by the Onsager-type dissociation of metastable geminate pairs. This process determines both the field and, together with intrinsic disorder, temperature dependences of the mobility.

A high carrier density can be reached without introducing counter charges due to either the field effect or high level of monopolar charge injection across a contact. Under these circumstances, the Coulomb interaction between carriers can also strongly change the effective potential landscape and even make it strongly fluctuating in time. However, the interaction between charges of the same sign is repulsive and, therefore, cannot create Coulomb traps. Instead, it gives rise to fluctuating in time potential barriers that still affect the mobility although this effect is significantly weaker than the effect of Coulomb traps. The broadening of the DOS distribution is, therefore, much smaller and the width of its deeper tail is affected much more weakly.

### Doping-induced broadening of the DOS distribution

An ionized dopant, embedded in a random network of localized states, affects the energy of nearby hopping sites due to Coulomb interaction of the dopant with charge carriers localized in those sites. For a given hopping site, the probability density,  $w(r)$ , of having a nearest dopant ion at a distance  $r$  is determined from the Poisson distribution as

$$w(r) = 4\pi r^2 N_d \exp\left(-\frac{4\pi}{3} N_d r^3\right), \quad (21)$$

where  $N_d$  is the concentration of ionized dopant atoms. A carrier, trapped by this localized state, will coulombically interact with the dopant ion and the potential energy of this interaction,  $E_c$ , is,

$$E_c = -\frac{e^2}{4\pi\epsilon_0\epsilon r} \quad , \quad (22)$$

with  $e$  being the elementary charge,  $\epsilon_0$  the dielectric permittivity, and  $\epsilon$  the relative dielectric constant. This energy, added to the intrinsic disorder energy,  $E_i$ , yields the total energy  $E$  of the hopping site:  $E = E_c + E_i$ . In the present work, we consider a relatively weak doping when the concentration of dopant ions remains much smaller than the total density of intrinsic hopping sites,  $N_i$ . Under these conditions, the energy of almost every localized state will be essentially affected only by the nearest dopant ion. Combining Eqs. (21) and (22) yields a distribution of the localized states over the Coulomb binding energy,  $g_c(E_c)$ . The result reads:

$$g_c(E_c) = w[r(E_c)] \left| \frac{dr}{dE_c} \right| = \frac{4\pi e^6 N_d}{(4\pi\epsilon_0\epsilon)^3 E_c^4} \exp \left[ \frac{4\pi N_d}{3} \frac{e^6}{(4\pi\epsilon_0\epsilon E_c)^3} \right] \quad . \quad (23)$$

The distribution of hopping sites over the total energy must account for both the intrinsic DOS  $g_i(E_i)$  and the distribution over the Coulomb energy  $g_c(E_c)$  given by Eq. (23). Integrating over  $E_c$  and  $E_i$  with the condition  $E_c + E_i = E$  leads to the following expression for the energy distribution function  $g(E)$  in a doped material

$$g(E) = \frac{4\pi e^6 N_d}{(4\pi\epsilon_0\epsilon)^3} \int_{-\infty}^0 \frac{dE_c}{E_c^4} \exp \left[ \frac{4\pi N_d}{3} \frac{e^6}{(4\pi\epsilon_0\epsilon E_c)^3} \right] \int_{-\infty}^{\infty} dE_i g_i(E_i) \delta(E - E_c - E_i) \quad , \quad (24)$$

where  $\delta$  is the Dirac delta function. Evaluating the integral over  $E_i$  in the right-hand side of Eq. (24) yields:

$$g(E) = \frac{4\pi e^6 N_d}{(4\pi\epsilon_0\epsilon)^3} \int_{-\infty}^0 \frac{dE_c}{E_c^4} \exp \left[ \frac{4\pi N_d}{3} \frac{e^6}{(4\pi\epsilon_0\epsilon E_c)^3} \right] g_i(E - E_c) \quad . \quad (25)$$

It is worth noting that Eq. (25) ignores both the Coulomb interaction between mobile charge carriers and contributions of non-nearest dopant ions to the Coulomb energy of localized states. At low dopant concentrations, the validity of this approximation is obvious. It can be also justified in heavier doped materials because dopant ions and carriers form relatively short pairs. Dipole moments of these pairs do affect the potential energy of more distant carriers but this effect is weaker as compared to the interaction with the nearest dopant ion. This argument is not, of course, valid in very heavily doped amorphous materials in which  $N_d$  approaches  $N_i$  and different pairs start to overlap. Since the value of  $N_i$  in disordered organic semiconductors is typically around  $10^{20} \dots 10^{21} \text{ cm}^{-3}$  the formulated model is applicable at dopant concentrations up to  $10^{18} \dots 10^{19} \text{ cm}^{-3}$ .

The effect of doping on an intrinsically Gaussian DOS distribution is shown in Fig. 8 for several doping levels. An increasing concentration of dopant ions converts increasingly large number of shallow sites into deep states. One should, therefore, expect that the doping-induced change in the DOS distribution would immediately affect the carrier hopping mobility. However, the density of mobile carriers also increases upon doping. Under equilibrium conditions, these carriers fill deep states and lift up the quasi-Fermi energy. For a fixed DOS distribution, this would lead to a higher average hopping rate and, concomitantly, higher carrier mobility. Thus, the mobility is determined by the interplay of two competing doping-induced processes. On the one hand, increasing density of mobile majority carriers shifts their energy distribution over localized states towards shallower sites, which facilitates the mobility. On the other hand, the Coulomb interaction with localized dopant ions of the opposite polarity effectively raises the density of states in the deep

tail of the DOS distribution and produces additional deep traps, which suppresses the jump rate and reduces the mobility. Below, we show that this interplay may lead to a non-monotonic dependence of the mobility upon the dopant concentration.

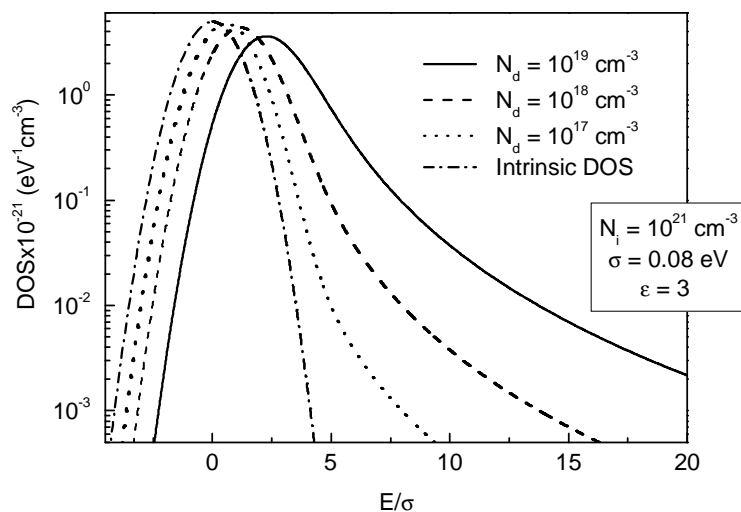


Fig. 8. The effect of doping on the DOS distribution in a disordered organic semiconductor. The Coulomb interaction between ionized dopants and charge carriers creates additional deep traps and broadens the deep tail of the DOS.

### Hopping in a doped organic semiconductor

At first glance, the calculation of the carrier mobility in a doped hopping system is straightforward: One may just use the doping-modified DOS distribution, given by Eq. (25), in the equations of the variable-range hopping model. However, this simple approach would significantly overestimate the role of the dopant-induced deep Coulomb traps. The reason is that the DOS itself does not contain information about correlations between energies and positions of the localized states. Since typical Onsager radius of a single Coulomb trap in an organic material is 10 to 20 nm and this trap consists of several hundreds of hopping sites, the correlations are essential as far as the carrier release from such a trap is concerned.

The energetic requirements for dissociative doping by an originally originally neutral dopant will be discussed first. Experimentally, it is known that an impurity can serve as, for instance, an electron acceptor in an organic semiconductor even if the LUMO of the dopant is  $\sim 1$  eV above the HOMO of the host molecules. Intuitively, it is not clear how the charge transfer can occur from a host molecule to a dopant under such circumstances. In order to clarify the situation one should bear in mind that both HOMO and LUMO energies are defined for isolated charges disregarding Coulomb interactions and/or intrinsic fields. However, in amorphous organic materials, charge transfer from a host molecule to a dopant should directly produce a strongly Coulombically bound short geminate pair rather than a free carrier. The size of such a pair is equal to the inter-molecular distance that is typically 0.6...1.0 nm. The Coulomb binding energy of this pair is then 0.5...0.8 eV if the permittivity retains its typical macroscopic value of 3 and 0.8...1.2 eV if the permittivity goes down to 2 at such short distances. If this energy gain is sufficient to compensate for the charge transfer energy, the geminate pair of charges rather than a neutral dopant and a neutral host molecule will form the ground state in a doped material.

Even if a carrier has been transferred from a dopant to a host molecule it cannot immediately contribute to the dc conductivity due to the Coulomb interaction that still bounds it to the parent dopant ion. A carrier can be released from a Coulomb trap in the course of a multi-jump Onsager-like process facilitated by the external electric field. Exact analytic consideration of this process, including correlations between energies and positions of hopping sites within Coulomb potential

wells, is hardly possible and one has to formulate a simplified model that still retains essential details of the carrier kinetics. We suggest a model based on the following simplifications: (i) every collective Coulomb trap surrounding a localized counter ion is replaced by a single deep localized state nearest to the ionized dopant and (ii) the energy of this site is a sum of the intrinsic disorder energy and the electrostatic energy  $\Delta$  counted from the top of the potential barrier which is formed by the Coulomb and external fields as

$$\Delta = \sqrt{\frac{e^3 F}{\pi \epsilon_0 \epsilon}} - \frac{e^2}{4\pi \epsilon_0 \epsilon a} \quad (26)$$

Under these assumptions the effective DOS distribution in a doped material takes the form

$$g(E) = \frac{N_i - N_d}{N_i} g_i(E) + \frac{N_d}{N_i} g_i\left(E + \frac{e^2}{4\pi \epsilon_0 \epsilon a} - \sqrt{\frac{e^3 F}{\pi \epsilon_0 \epsilon}}\right) \quad (27)$$

A model of variable-range hopping in a disordered material at a finite carrier density has been formulated in Refs. [17,22]. This model is based on the concept of the effective transport energy [8,9,23] that virtually reduces the problem to trap-controlled transport with a broad energy distribution of localized states [19]. In the following we always assume that the material is macroscopically neutral, i.e. that the average density of carriers is equal to the concentration of dopants. The field dependence of the mobility, calculated with the DOS distribution given by eq. (27) at a moderate concentration of dopants  $N_d = 10 \text{ cm}^{-3}$ , is shown in Fig. 9 parametric in temperature. A Gaussian distribution of the width  $\sigma = 100 \text{ meV}$  has been used as an intrinsic DOS distribution. Although the curves follow the Poole-Frenkel type  $\log \mu \propto F^{1/2}$  dependence at weaker fields they tend toward saturation at stronger fields. Fig. 10 illustrates the temperature dependence of the mobility at different external fields. Although both the doping-induced Coulomb traps and the intrinsic DOS distribution affect this dependence most carriers are localized in the former, which gives rise to an almost perfect Arrhenius temperature dependence with the slope affected by the external field. As shown in the inset to Fig. 10, an attempt to visualize these data on a  $\log \mu$  vs  $1/T^2$  plot fails to yield straight lines indicating that the mobility is effectively controlled by carrier jumps from states around the Fermi level [17,22]. One should expect that, at lower temperatures, the effective transport level should approach the Fermi level, and the temperature dependence of the mobility has to almost level off featuring the Mott  $T^{-1/4}$  law.

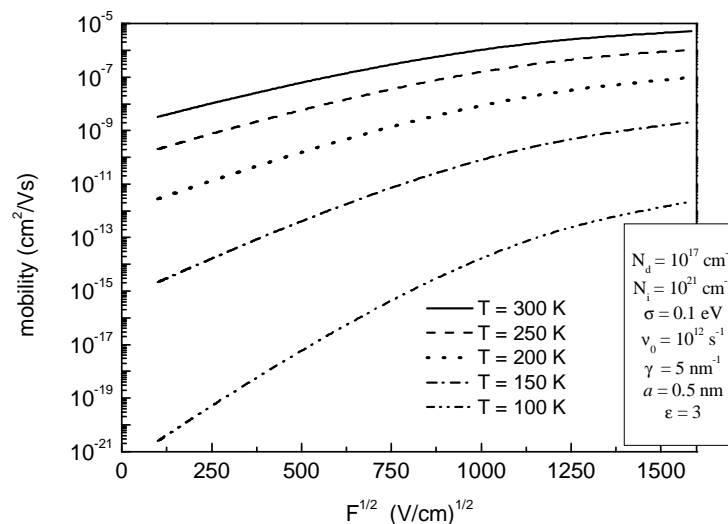


Fig. 9. Field dependences of the charge carrier mobility in a doped disordered organic semiconductor at different temperatures.

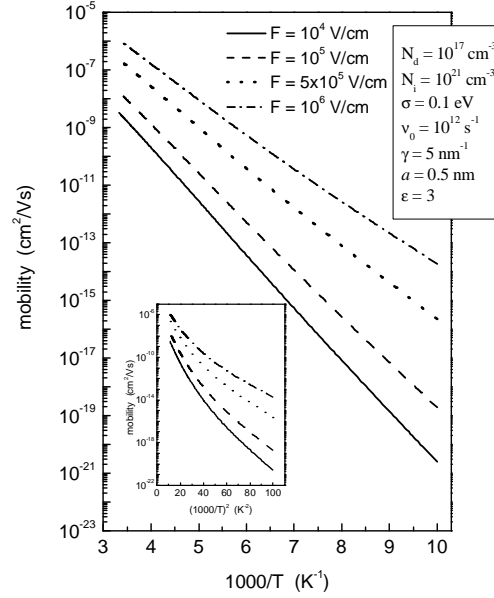


Fig. 10. Temperature dependence of the mobility in a doped disordered organic material. The inset shows the same set of curves replotted in  $\log \mu$  vs  $1/T^2$  axes.

Fig. 11 illustrates the dopant concentration dependence of the mobility parametric in the width of the intrinsic Gaussian DOS distribution. These dependencies are strikingly different in materials with weak and strong energy disorder, i.e. with small and large values of the DOS width. While doping a weakly disordered system suppresses the mobility the latter increases with doping level in strongly disordered materials. It should be, however, noted that the mobility always decreases with doping more weakly than  $1/N_d$  and, therefore, the conductivity, which is proportional to the product of  $\mu$  and  $N_d$ , increases upon doping even in materials with small DOS widths.

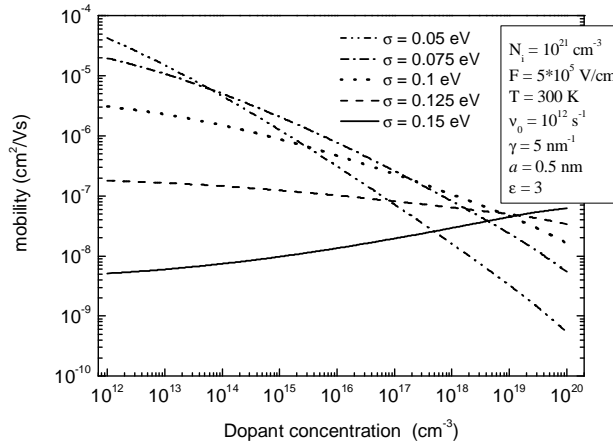


Fig. 11. Dependence of the carrier mobility upon the concentration of dopants in materials with different variations of the intrinsic DOS distribution.

In order to understand why the mobility in weakly and strongly disordered materials is so differently affected by doping one should bear in mind that dopants provide both charge carriers and deep Coulomb traps. If these traps are deeper than those states that control the mobility in the pristine material, the deep Coulomb traps will still trap majority of doping-induced carriers and their mobility has to be smaller than the carrier mobility in the undoped material. The electrostatic energy of a Coulomb trap can be estimated from Eq. (26) as 0.5 eV in a field of 1 MV/cm with  $a = 0.5$  nm and  $\epsilon = 3$ . However, the effective depth of a Coulomb trap is smaller due to the fact that carriers can escape from this trap by jumps via localized states with energies below the maximum of the DOS

distribution. [8,9,17,22,23] The activation energy of the mobility can be estimated from the curves plotted in Fig. 10 and for the field of 1 MV/cm this energy is only 0.36 eV.

In a pristine material with a Gaussian DOS the distribution of localized carriers has a maximum at the energy  $E_m$  of  $\sigma_i^2/kT$  below the maximum of the intrinsic DOS function. In a strongly disordered material with  $\sigma_i = 120$  meV the energy  $E_m$  is as large as 0.6 eV at room temperature. This energy is larger than the activation energy of the Coulomb traps and carriers can easily leave the latter and fill the deep tail of the intrinsic DOS at energies below and *above*  $E_m$ . Concomitantly, the Fermi level elevates which leads to increasing mobility upon doping. In other words, disordered organic materials can be efficiently doped by introducing virtually deep Coulomb traps because free equilibrated carriers fill states in the deep tail of the intrinsic DOS distribution that are even deeper than the Coulomb traps.

If the activation energy of the dopant-induced Coulomb traps is larger than  $E_m$  most doping-induced carriers are still localized within Coulomb potential wells of ionized dopants and in the deep tail states *below*  $E_m$ . The dominant effect of doping is then creation of additional deep states in the DOS and, concomitantly, the mobility decreases with increasing  $N_d$ . However, this decrease is weaker than  $1/N_d$  and the conductivity, determined by the product of the mobility and carrier density, still increases with increasing dopant concentration.

It is known from both experimental studies and theoretical considerations that the mobility must strongly increase at high doping levels [14,17,18]. However, this effect cannot be analyzed within the framework of the present model because the latter is valid only at relatively low doping levels when the Coulomb potential wells of ionized dopants do not overlap. The increase of the mobility at high values of  $N_d$  is associated with filling of deep tail states by carriers. This is possible only if adding new dopants do not create new deep Coulomb traps, which is the case at very high dopant concentration when Coulomb potential wells already strongly overlap and additional ionized dopants smoothen rather than roughen the potential landscape. [17]

Since the effective depth of Coulomb traps is controlled by the external field, one should expect different dopant-concentration dependencies of the mobility at weak and strong electric fields. This effect is illustrated in Fig. 12. Indeed, at weak external fields, Coulomb potential wells are deep and ionized dopants serve as deep traps for carriers. Strong external fields reduce the barrier for carrier release from Coulomb traps making them shallower and, thereby, increasing the density of free carriers and the average carrier mobility. It is interesting that the effect of the external field on the effective depth of a Coulomb trap does not depend upon the field direction. Therefore, carriers in the channel of an organic field-effect transistor should not experience the Coulomb trapping by dopant ions due to a strong vertical field and their mobility along the channel should increase with doping level even if the lateral field is weak.

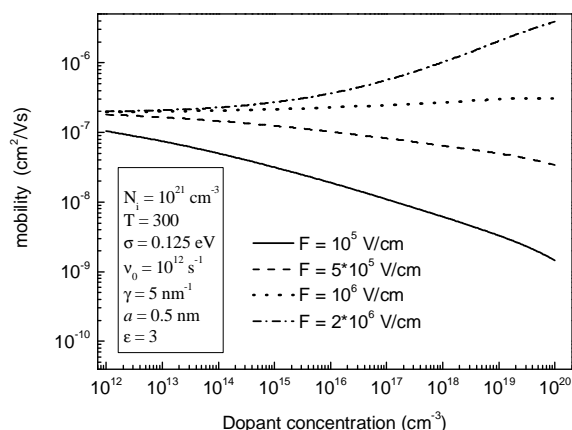


Fig. 12. Dependence of the carrier mobility upon the concentration of dopants at different external fields.

The zero-field activation energy of a Coulomb trap strongly depends upon the distance  $a$  between an ionized dopant and the nearest intrinsic hopping site, i.e. upon the size of the equilibrium dark ‘geminate pair’ formed by the dopant ion and a charge carrier occupying the nearest site.

Concomitantly, this parameter controls the critical value of the external field at which the negative dopant-density dependence of the mobility is changed to positive. The field dependences of the mobility are shown in Fig. 13 for different sizes of the dark geminate pairs. As one could anticipate, the critical value of the field, at which the effect of Coulomb traps vanishes and the mobility saturates, strongly increases with decreasing  $a$ .

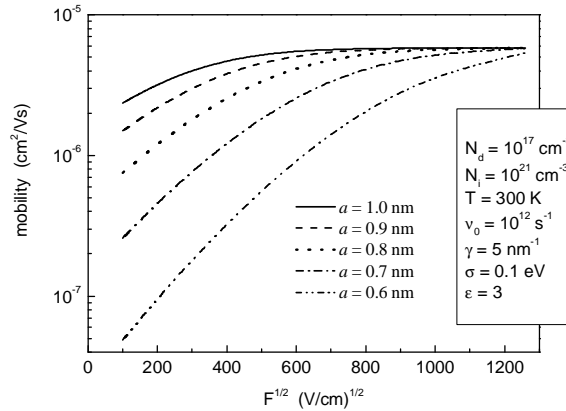


Fig. 13. Field dependences of the mobility calculated for different distances between the dopant ions and nearest hopping sites, i.e. for different effective depths of the Coulomb potential wells.

It should be noted that all our calculations have been done for a fixed size of the dark geminate pairs. However, one should expect a distribution of the parameter  $a$  in a disordered material. The curves shown in Fig. 14 were calculated for the following normalized Gaussian distribution,  $f(a)$ , of pair sizes

$$f(a) = 8\sqrt{\frac{2}{\pi}} \frac{a^2}{a_0^3} \exp\left(-\frac{a^2}{2a_0^2}\right), \quad (28)$$

where  $a_0$  is the width of the distribution. The value of  $a_0 = 0.2$  nm was used in the calculations. With this value of  $a_0$ , the function  $f(a)$  has a maximum at  $a \approx 0.5$  nm, i.e. at the same pair size as has been used in the mobility calculations with a fixed value of  $a$  see e.g. Fig. 9. Since larger values of  $a$  correspond to shallower Coulomb traps larger pairs give a major contribution to the mobility at weaker fields. Concomitantly, the weak-field mobility is higher in a material with a distribution of pair sizes. Very deep Coulomb traps, formed by short pairs, can keep carriers even at strong fields and, therefore, the strong-field mobility turns out to be smaller in materials with varying sizes of charge-dopant pairs. As a result, the slope of the  $\log \mu$  vs  $F^{1/2}$  curves decreases as compared to those calculated with a fixed value of  $a$ .

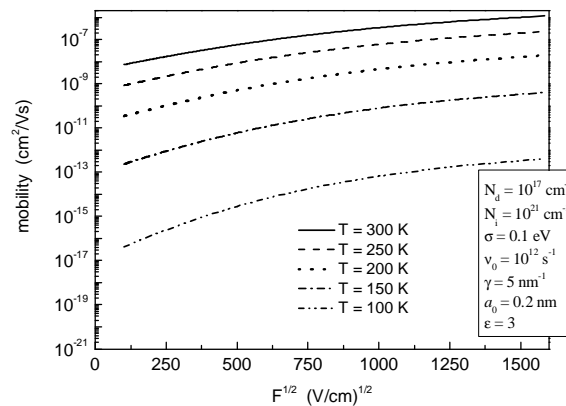


Fig. 14. Field dependences of the mobility calculated for different widths of the Gaussian distribution of distances between the dopant ions and nearest hopping sites.

It should be noted that the result, discussed above, were obtained under the assumption that the density of charge carriers is equal to the density of dopants, i.e. that the field-driven carrier ejection from a sample is fully compensated by charge injection and *vice versa*. This condition can be violated if a blocking contact is used, which is typical for the time-of-flight (TOF) measurements. Upon application of an external electric field all mobile carriers will sooner or later be extracted from the sample and only Coulomb traps surrounding counter ions will remain in the bulk. In a heavily doped material this will result in the formation of a zone at the blocking contact that is depleted of mobile carriers. However, in an accidentally doped (apparently pristine) material with a low density of dopant ions the field can still remain almost constant. In order to simulate the TOF mobility, measured in such samples, one has to use the DOS distribution given by Eq. (27) and assume the density of photogenerated carriers much smaller than the dopant concentration. The use of this model yields the mobility that is orders of magnitude smaller than at higher carrier densities and reveals a perfect Poole-Frenkel field dependence within the entire field range as illustrated in Fig. 15. This result offers a plausible explanation of the notorious difference [17,18] between both the magnitudes and field dependences of the field-effect and space-charge-limited-current mobility, on the one hand, and the mobility measured in TOF experiments, on the other.

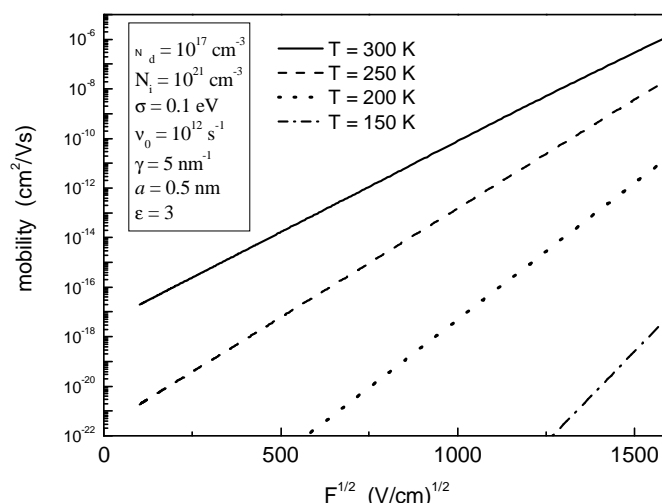


Fig. 15. Field dependences of the single-carrier (TOF) carrier mobility in a doped disordered organic material at different temperatures.

In conclusion to this section: it is shown that the density of states distribution in a disordered organic semiconductor is strongly affected by doping. Due to the Coulomb interaction between released charge carriers and ionized dopants the deep tail of the intrinsically Gaussian DOS distribution broadens and the total density of deep localized states strongly increases with increasing dopant content. Therefore, doping of a disordered organic semiconductor, on the one hand, increases the concentration of charge carriers and lifts up the Fermi level but, on the other hand, creates deep Coulomb traps. While the former effect facilitates conductivity, the latter strongly suppresses the carrier hopping rate. The trade-off between increasing densities of both charge carriers and Coulomb traps is controlled by the intrinsic DOS width and external field strength. In strongly disordered materials and/or at strong electric fields, the carrier mobility increases with increasing dopant concentration. Otherwise, carrier localization in Coulomb potential wells takes over and the mobility decreases upon doping. The TOF measurements in intentionally or accidentally doped samples yield the Poole-Frenkel-like field dependence of the mobility that is orders of magnitude smaller than the mobility measured at high carrier densities.

### 3. Space charge limited currents in organic materials with a Gaussian density-of-states distribution

If a current-voltage (IV) characteristic of an organic light-emitting diode (OLED) or an organic thin-film transistor has to be analyzed, the first question to be answered is whether the current is controlled by space charge in the bulk or by charge injection from the contact. It is generally believed that the current in an organic device is limited by injection if the zero-field contact barrier is higher than 0.25-0.30 eV [16]. At lower barriers, one should expect the regime of space charge limited current (SCLC) [19] [24]. In other words, the barrier height has been commonly considered as the only parameter that universally determines the relative contributions from the injection and space charge effects to the observed IV characteristics irrespective of the temperature and bias.

In order to analyse the interplay between charge injection and bulk conductivity one must use specific models for both injection and SCLC. Variable range carrier hopping in a positionally random and energetically disordered system of localized states has been since long recognized as the dominant charge transport mode in amorphous organic semiconductors and polymers [16,3]. Recently, it has been shown that a similar hopping approach yields a quantitatively correct description of the field and temperature dependences of the rate of charge injection across a metal/polymer interface [25,26]. Since the field and temperature dependences of the hopping injection limited current (ILC) and hopping SCLC are different, one can expect that, at a fixed zero-field barrier height, the conductivity can be determined by either ILC or SCLC depending upon the bias and temperature.

The hopping model [25,27,28] considers charge injection across a metal/polymer interface as a two-step process. Firstly, carriers jump from the Fermi level of a metal contact into localized states that are sufficiently close to the interface and, therefore, can be reached directly from the contact. Every injected carrier will immediately create an image charge of the opposite sign at the contact. The superposition of the external field at the contact,  $F_0$ , and the Coulomb field of the image charge form the potential well,

$$U(x) = \Delta - \frac{e^2}{16\pi\epsilon_0\epsilon x} - eF_0x \quad ,$$

for the charge carrier localized near the interface, where  $\Delta$  is the zero-field barrier height. Carrier hopping within this potential well results in either neutralization at the contact or crossing of the potential barrier and penetration into the bulk as described by the one-dimensional version of the Onsager theory [21]. Combining the rate of first jumps with the Onsager escape probability one arrives at the following expression [25,28] for the total hopping injection current,  $j_{inj}$ ,

$$j_{inj} = e\nu^a \frac{\int_0^\infty dx_0 \exp(-2\gamma x_0) \int_{-\infty}^\infty dE \text{Bol}(E) g[E - U(x_0)] \int_a^{x_0} dx \exp\left[-\frac{e}{kT}\left(F_0x + \frac{e}{16\pi\epsilon_0\epsilon x}\right)\right]}{\int_a^\infty dx \exp\left[-\frac{e}{kT}\left(F_0x + \frac{e}{16\pi\epsilon_0\epsilon x}\right)\right]} \quad , \quad (29)$$

where  $\nu$  is the attempt-to-jump frequency of carriers from the metal contact,  $a$  the distance from the electrode to nearest hopping sites inside the polymer,  $T$  the temperature,  $k$  the Boltzmann constant,  $\gamma$  the inverse localization radius, and  $g(E)$  the density-of-states (DOS) distribution. The function  $\text{Bol}(E)$  is defined as

$$\text{Bol}(E) = \begin{cases} \exp\left(-\frac{E}{kT}\right), & E > 0, \\ 1, & E < 0. \end{cases} \quad (30)$$

In order to fully describe the monopolar current in a polymer film, one has to combine the above expression for the charge injection rate with the equations describing SCLC in organic materials. The transport model must be based on the variable-range hopping within a random system of localized states characterized by a Gaussian DOS energy distribution function. The SCLC, controlled by a Gaussian distribution of localized states, was earlier considered within the framework of the multiple-trapping model [29,13]. It has been also recognized that the variable range hopping is mathematically equivalent to the trap-controlled band transport with the so-called effective transport energy,  $E_{tr}$  (eq. (10)), playing the role of the mobility edge and the effective ‘free carrier’ mobility determined by the rate of carrier jumps between hopping sites of energies around  $E_{tr}$  [8, 9].

The equation, relating the equilibrium energy distribution of localized carriers,  $\rho(E,x)$ , and the density of ‘mobile’ carriers,  $n_m(x)$ , occupying hopping sites around the effective transport level, then takes the form

$$\frac{g(E) - \rho(E,x)}{N_t} n_m(x) - \exp\left(-\frac{E_{tr} - E}{kT}\right) \rho(E,x) = 0 \quad . \quad (31)$$

The total carrier density  $n(x)$  and the electric field  $F(x)$  are related by the Poisson equation,

$$\frac{dF(x)}{dx} = \frac{e}{\epsilon_0 \epsilon} n(x) \quad . \quad (32)$$

The current density  $j$  is determined by the density of ‘mobile’ carriers and their mobility  $\mu$  as,

$$j = e\mu F(x) n_m(x) \quad . \quad (33)$$

It is worth noting that carriers, occupying hopping sites around  $E_{tr}$ , mostly jump down to deeper states and, therefore, their mobility can only weakly depend upon temperature [23]. In amorphous materials with a high density of localized states, the total carrier density is practically equal to the density of localized carriers:

$$n(x) = \int_{-\infty}^{E_{tr}} dE \rho(E,x) \quad . \quad (34)$$

In order to fully account for the interplay between the charge injection and the space charge effects one should solve Eqs. (31)-(34) with the boundary condition given by Eq. (29) in which  $F_0$  has to be considered as the field at the injecting contact:  $F_0 = F(0)$ .

Solving Eq. (31) for the function  $\rho(E,x)$  and substituting this solution into Eq. (34) yields the following equation relating the total carrier density and the density of ‘mobile’ carriers,

$$n(x) = \int_{-\infty}^{E_{tr}} \frac{dE g(E)}{1 + \exp\left[\frac{E - E_F(x)}{kT}\right]} \quad , \quad (35)$$

with the Fermi energy  $E_F(x)$  being determined by the density of ‘mobile’ carriers or, equivalently, by the field and current as described by Eq. (33):

$$E_F(x) = kT \ln \left[ \frac{n_m(x)}{N_t} \right] = kT \ln \left[ \frac{j}{e\mu F(x) N_t} \right] \quad . \quad (36)$$

Combining Eqs. (32), (35), and (36) yields the equation for the field distribution,

$$\frac{dF(x)}{dx} = \frac{e}{\epsilon_0 \epsilon} \int_{-\infty}^{E_x} dE g(E) \left[ 1 + \frac{e \mu V_0 \tau_0 N_t}{j} F(x) \exp\left(\frac{E}{kT}\right) \right]^{-1}. \quad (37)$$

In order to calculate the hopping IV characteristics one must solve Eq. (37) together with the injection boundary condition,  $j = j_{inj}(F_0)$  with  $F_0 = F(0)$ . It should be noted that the image-charge potential is not included into Eq. (37). This potential is very important for charge injection but it extends for only 10 nm or less into the bulk while the sample thickness,  $L$ , is typically 100 nm or more.

Below, the results of the calculation will be illustrated for the Gaussian DOS distribution of Eq.(12), with density of hopping sites  $N_t$ . The calculated spatial dependence of the field is shown in Fig. 16 for different heights of the injection barrier  $\Delta$ . In accordance with what one should expect, the field remains almost constant at high injection barriers while a strongly inhomogeneous space charge controlled field distribution has been obtained at lower barriers. For the invoked set of material parameters, the onset of SCLC regime corresponds to the barrier height of  $0.2 \div 0.3$  eV.

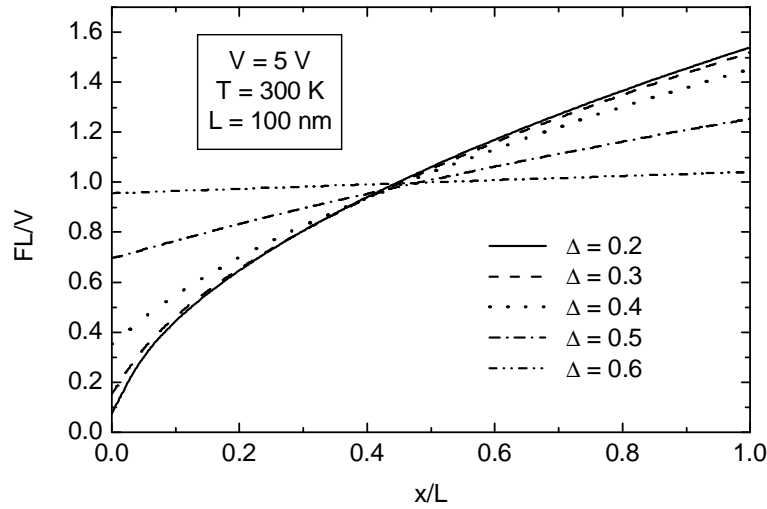


Fig. 16. Spatial distribution of the electric field at different heights of the injection barrier calculated for the following material parameters:  $\nu = 10^{14} \text{ s}^{-1}$ ,  $N_t = 5 \times 10^{20} \text{ cm}^{-3}$ ,  $\sigma = 0.1 \text{ eV}$ ,  $\gamma = 5 \text{ nm}^{-1}$ .

However, the injection barrier height is not the only parameter that controls the charge transport mode. An interesting feature of the hopping injection is an anomalously weak temperature dependence that can be observed even if the zero-field contact barrier  $\Delta$  is high. The  $T$ -dependence of the injection current is illustrated in Fig. 17 for different barrier heights together with the temperature dependence of the hopping SCLC calculated for the same set of material parameters. The latter dependence turns out to be much steeper although the invoked DOS width of 0.1 eV is much smaller than the injection barrier heights. This fact indicates a possibility of the crossover from a ILC to SCLC with decreasing temperature irrespective of the injection barrier height. For every particular value of  $\Delta$ , SCLC can be dominant at sufficiently low temperatures although the crossover temperature decreases with increasing  $\Delta$ .

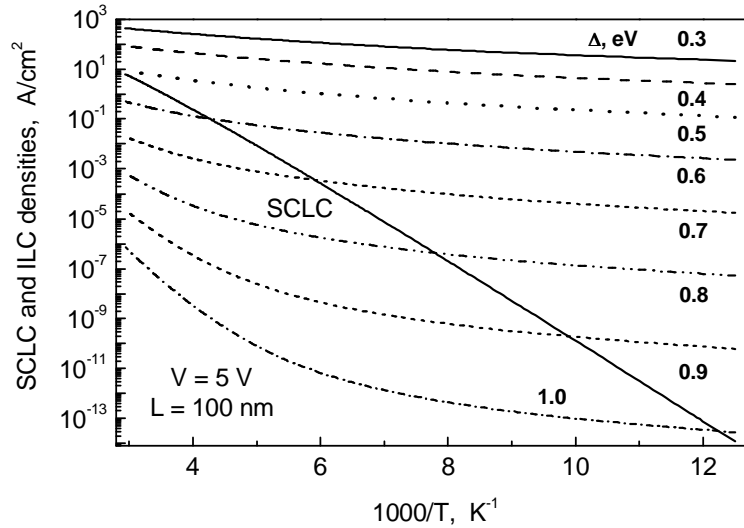


Fig. 17. Temperature dependences of SCLC and ILC. Material parameters are listed in the capture to Fig. 16.

The IV characteristics, shown in Fig. 18, are calculated at three different temperatures (i) from Eq. (29) assuming injection-limited charge transport, (ii) from Eq. (37) with  $F(0) = 0$  assuming 'pure' SCLC, and (iii) from Eq. (37) with the boundary condition for the field given by Eq. (29), i.e. with the full account for both injection and space charge limitations. Since the injection rate only weakly decreases with temperature the low-temperature IV characteristics are fully controlled by the space charge in the bulk even if the injection barrier is as high as 0.7 eV. With increasing temperature, SCLC increases much stronger than ILC and the latter almost fully determines IV characteristics at higher temperatures. At intermediate temperatures, one can obtain a combined IV characteristic that is controlled by the space charge at low and high voltages and by the rate of carrier injection at moderate biases.

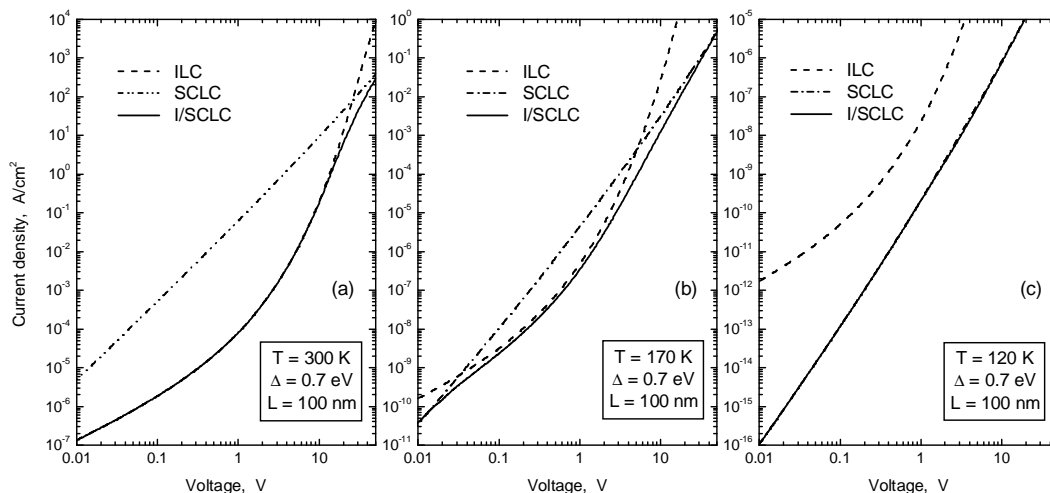


Fig. 18. Current-voltage characteristics of ILC, SCLC, and the current, controlled by both injection from the contact and space charge in the bulk. The set of material parameters is the same as in Fig. 16.

#### 4. Equilibrium hopping mobility of polarons in disordered organic materials

Polaron effects on charge carrier transport in both organic and inorganic materials were extensively discussed in the literature during last two decades [16, 30-33]. The small polaron model [31,32] was often exploited, implying that a localized carrier is strongly coupled either to local polarization or to vibrations and/or rotations of the molecule at which it resides. These processes cause carrier self-trapping and create a quasi-particle, a polaron, which can move only by carrying along the associated structural deformation. The adiabatic zero-field activation energy of the polaron mobility is  $E_p/2$ , where  $E_p$  is the polaron binding energy [16].

The model of trap-controlled transport with monoenergetic traps predicts exactly the same temperature dependence of the mobility if the energy of traps is equal to  $E_p/2$ . The occurrence of a single trapping level is typical for crystalline materials with defects or impurities. Therefore, it is notoriously difficult to distinguish between the mobility controlled by the polaron formation and the mobility controlled by monoenergetic traps. In disordered materials, both polaron formation and carrier trapping by either defects or impurities occur on the background of a broad distribution of either band-tail states or transport hopping sites. It was demonstrated [34-36] that the interplay between the polaronic and disorder effects may be responsible for the specific temperature dependence observed in some amorphous materials. Bässler *et al.* [35] suggested that the effective zero-field activation energy,  $E_a^{(eff)}$ , of the mobility in a random hopping system with a Gaussian density-of-states (DOS) distribution can be approximated by a sum of the disorder and polaron contributions as,

$$E_a^{(eff)} = E_a^{(p)} + E_a^{(d)} = \frac{E_p}{2} + \frac{4\sigma^2}{9kT} \quad , \quad (38)$$

where  $E_a^{(p)}$  and  $E_a^{(d)}$  are the polaronic and disorder contributions, respectively,  $\sigma$  is the width of the DOS distribution,  $T$  the temperature, and  $k$  the Boltzmann constant. Since  $E_p$  is mostly determined by short-range relaxations it is not affected by the medium- and long-range disorder and can be considered as a well-defined material parameter, which is not subjected to distribution. We consider the polaron effect and the effect of monoenergetic traps on hopping charge carrier transport in disordered materials.

The rate  $\nu$  of a tunneling carrier jump over the distance  $r$  between an initially occupied hopping site of the energy  $E_{st}$  to a vacant target site of the energy  $E_t$  is usually described by the Miller-Abrahams expression [4] (Eq (1)). It is worth noting that the energy  $E_{st}$  accounts for the polaron binding energy as:  $E_{st} = E - (E_p/2)$ . If a carrier occupies a sufficiently deep localized state it can hardly find a nearby hopping site that is even deeper than the occupied site. Therefore, a next jump of this carrier will, most probably, be an energetically upward jump. The rate of such jumps is determined by the trade-off between the distance to a vacant site and the energy difference between starting and target sites,  $E_t - E_{st}$ .

The Mott theory of the variable range hopping [37] considers the interplay between jump distance and the energy difference for carrier jumps within a constant DOS distribution around the Fermi level. Under these conditions, the energy of the most probable target site depends upon the starting site energy. However, if the DOS function steeply increases with energy most upward carrier jumps will be made to target sites whose energies do not depend upon energies of starting sites [8,9]. As pointed out in a previous section, this implies the occurrence of a universal energy level of most probable jumps, called the effective transport level,  $E_{tr}$ , in a disordered hopping system. This level effectively plays the role of the mobility edge in disordered materials with trap-controlled band carrier transport. The major difference between the mobility edge and the effective transport level is that the former is normally considered as a material parameter while the latter depends upon temperature and external electric field. Below we consider carrier hopping at weak electric fields, which allows neglecting the field effect on  $E_{tr}$ .

The traditional Mott approach was applied to the calculation of the effective transport energy in random hopping systems with an exponential [9,38] and a Gaussian [39] DOS distribution.

The temperature and concentration dependencies of  $E_{tr}$  obtained for an exponential DOS [9,38] are in good qualitative agreement with the predictions of both Monte Carlo simulation [8] and analytic models [40]. However, for a Gaussian DOS it was surprisingly found that, at higher temperatures, most carriers will jump to sites above the maximum of the DOS distribution [39]. This, obviously, implies that the Mott approach to the variable-range hopping is not directly applicable to the calculation of the effective transport energy. Therefore, in the present calculation we follow the method described earlier for the calculation of  $E_{tr}$  in hopping systems with non-constant DOS distributions [23].

The equilibrium energy distribution of localized carriers is determined by the Boltzmann function independent of the dominant carrier transport mode. Therefore, the normalized carrier distribution function,  $f(E_s)$ , in a hopping system can be written as,

$$f(E_s) = \left[ \int_{-\infty}^{\infty} dE_s g(E_s - (E_p/2)) \exp\left(-\frac{E_s}{kT}\right) \right]^{-1} g(E_s - (E_p/2)) \exp\left(-\frac{E_s}{kT}\right) . \quad (39)$$

The equilibrium carrier diffusivity,  $D$ , can be evaluated as the product of the average carrier jump rate  $\langle \nu \rangle$ ,

$$\begin{aligned} \langle \nu \rangle &= \nu_0 \int_{-\infty}^{E_{tr}} dE_s f(E_s) \exp\left(-\frac{E_{tr} - E_s}{kT}\right) = \\ &= \nu_0 \exp\left(-\frac{E_{tr}}{kT}\right) \left[ \int_{-\infty}^{\infty} dE_s g(E_s - (E_p/2)) \exp\left(-\frac{E_s}{kT}\right) \right]^{-1} \int_{-\infty}^{E_{tr}} dE g(E) = \\ &= \nu_0 \exp\left(-\frac{E_{tr} + (E_p/2)}{kT}\right) \left[ \int_{-\infty}^{\infty} dE g(E) \exp\left(-\frac{E}{kT}\right) \right]^{-1} \int_{-\infty}^{E_{tr}} dE g(E) \end{aligned} \quad (40)$$

and the average square jump distance,  $\langle r^2 \rangle$ ,

$$\langle r^2 \rangle = \left[ \int_{-\infty}^{E_{tr}} dE_t g(E_t) \right]^{-2/3} . \quad (41)$$

Under equilibrium conditions, one may use the Einstein relation between the mobility and diffusivity  $\mu = eD/kT$ , which yields

$$\mu = \frac{e\nu_0}{kT} \exp\left(-\frac{E_{tr} + (E_p/2)}{kT}\right) \left[ \int_{-\infty}^{\infty} dE g(E) \exp\left(-\frac{E}{kT}\right) \right]^{-1} \left[ \int_{-\infty}^{E_{tr}} dE g(E) \right]^{1/3} . \quad (42)$$

The Arrhenius-like factor  $\exp(-E_p/2kT)$  is the only difference between Eq. (42) and the expression for the equilibrium hopping mobility obtained in [41] neglecting polaronic relaxation. Therefore, Eq. (42) can be written as,

$$\mu = \mu_0 \exp\left[-\frac{E_a(T) + (E_p/2)}{kT}\right] , \quad (43)$$

where  $E_a$  is the activation energy of the carrier mobility in a hopping system with the same DOS distribution in the absence of the polaronic effect. Remarkably, this result is valid for an arbitrary

DOS distribution. Fig. 19 shows the temperature dependence of  $\mu$  in a material with a Gaussian DOS distribution of localized states subjected to polaronic relaxation.

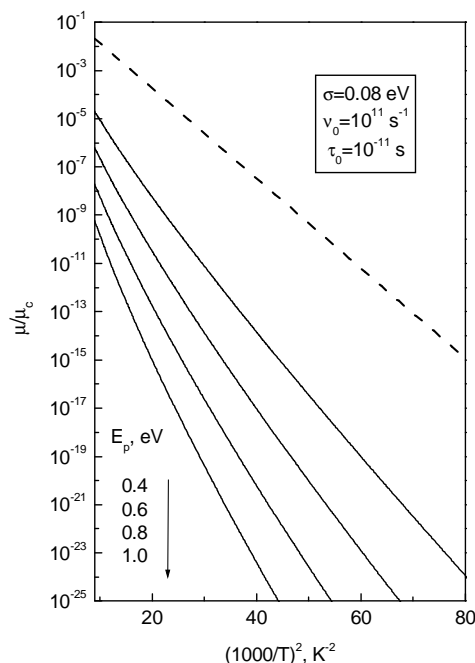


Fig. 19. The effect of polaron binding energy on the temperature dependence of the equilibrium trap-controlled carrier mobility in a disordered material with a Gaussian DOS distribution. The dashed line shows the mobility in the absence of the polaronic effect.

It is notoriously difficult to distinguish between the effects of polaronic relaxation and deep trapping on charge carrier transport characteristics [34,35]. Both effects lead to an Arrhenius-like contribution to the temperature dependences of the mobility, diffusivity, recombination rate, etc. Therefore, independent experimental evidence is essential in order to distinguish between deep trapping and polaronic relaxation. Particularly, the latter but not the former must lead to an unusually strong redshift of the photoluminescence spectrum with respect to the optical absorption edge. Below the effects of polaronic relaxation and deep trapping on the temperature dependence of the equilibrium trap-controlled carrier mobility are compared.

However, the fit of experimental data in terms of either deep trapping or polaronic effects can yield different sets of material parameters. In some cases the fitting parameters can turn out to be hardly realistic for one of the models, implying that the other one is more likely in a given material. Magin and Borsenberger [34] measured the electron time-of-flight mobility in N,N-bis(2-phenethyl)-perylene-3,4:9,10-bis(dicarboximide), hereafter PECl. On the basis of qualitative analysis of the data, they arrived at the conclusion that electronic transport in this material is affected by both the energy disorder and either polaron formation or carrier trapping. The above-formulated model of hopping transport of polarons does fit the temperature dependence of the carrier mobility in PECl. This fit is illustrated in Fig. 20 by the solid line calculated from Eq. (42) for a Gaussian DOS with  $\sigma = 57$  meV,  $N = 5 \times 10^{20}$  cm<sup>-3</sup>,  $\gamma = 4 \times 10^7$  cm<sup>-1</sup>, and  $E_p = 0.52$  eV. However, this fit requires an unreasonably high value of the attempt-to-jump frequency  $\nu_0 = 4 \times 10^{16}$  s<sup>-1</sup>. That large value of  $\nu_0$  is required in order to compensate for the Boltzmann exponential  $\exp(-E_p/2kT)$ , which accounts for the polaron activation energy.

The experimentally observed temperature dependence of the mobility can be equally well explained by deep carrier trapping. The hopping mobility in the presence of deep traps can also be calculated from Eq. (42) with  $E_p = 0$  and the DOS function that accounts for Gaussian distributions of both hopping sites and traps as,

$$g(E) = \frac{1}{\sqrt{2\pi}} \left\{ \frac{N_s}{\sigma_s} \exp\left(-\frac{E^2}{2\sigma_s^2}\right) + \frac{N_t}{\sigma_t} \exp\left[-\frac{(E + E_t)^2}{2\sigma_t^2}\right] \right\}, \quad (44)$$

where  $N_s$ ,  $N_t$  and  $\sigma_s$ ,  $\sigma_t$  are the densities and Gaussian widths of the hopping-site and trap distributions, respectively. The dashed line in Fig. 20 shows the temperature dependence of the mobility, calculated from Eqs. (42) and (44) with  $\sigma_s = 57$  meV,  $\sigma_t = 52$  meV,  $E_t = 0.295$  eV,  $N_s = 5 \times 10^{20}$  cm<sup>-3</sup>,  $N_t = 8 \times 10^{16}$  cm<sup>-3</sup>,  $\gamma = 10^7$  cm<sup>-1</sup>, and a quite reasonable value of  $\nu_0 = 2 \times 10^{13}$  s<sup>-1</sup>. The dashed and solid lines practically merge indicating that it is virtually impossible to distinguish between polaron formation and deep trapping on the basis of the fit quality except for the likelihood of the fitting parameters.

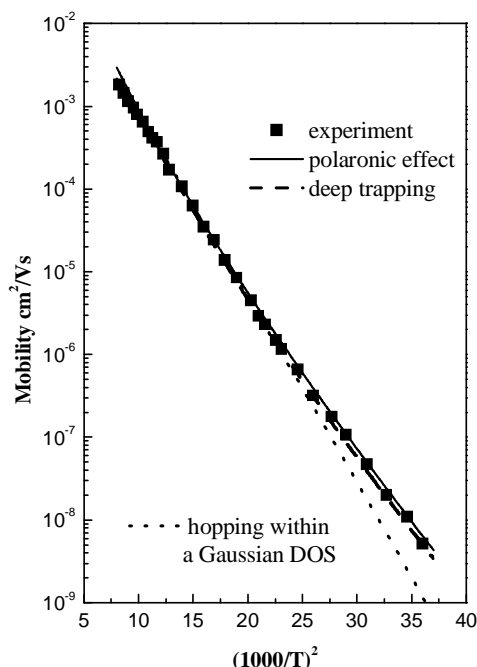


Fig. 20. Temperature dependence of the carrier mobility in Peci [31]. The solid and dashed curves are calculated taking into account the polaron formation and deep traps, respectively. The parameters used for the calculation are listed in the text. The dotted line shows the best fit of the data disregarding both the polaronic effect and deep carrier trapping with  $\sigma = 104$  meV,  $N = 5 \times 10^{20}$  cm<sup>-3</sup>,  $\nu_0 = 2 \times 10^{13}$  s<sup>-1</sup>, and  $\gamma = 3.3 \times 10^7$  cm<sup>-1</sup>.

The effect of polaronic relaxation on equilibrium charge carrier transport in disordered materials can be accounted for by simply adding a half of the polaron binding energy to the activation energy of equilibrium carrier mobility and/or diffusivity. Although it is really difficult to distinguish between the effects of polaron formation and deep trapping on the basis of the mobility measurements within a relatively narrow temperature range it can be done if the fitting parameters are physically unrealistic for one of these models. Otherwise, independent, e.g. spectroscopic, evidence is necessary in order to identify polarons as charge carriers in a disordered organic material.

## References

- [1] A. Dieckmann, H. Bässler, P. M. Borsenberger, *J. Chem. Phys.* **99**, 8136 (1993).
- [2] S. V. Novikov, A. V. Vannikov, *J. Phys. Chem.* **99**, 14573 (1995).
- [3] H. Bässler, *Phys. Stat. Sol. (b)* **175**, 15 (1993).

- [4] A. Miller, E. Abrahams, *Phys. Rev.* **120**, 745 (1960).
- [5] V. I. Arkhipov, G. J. Adriaenssens, *J. Phys.: Condens. Matter* **8**, 7909 (1996).
- [6] A. Kadashchuk, Yu. Skryshevskii, A. Vakhnin, N. Ostapenko, V. I. Arkhipov, E. V. Emelianova, H. Bässler, *Phys. Rev. B* **63**, 115205 (2001).
- [7] V. I. Arkhipov, E. V. Emelianova, H. Bässler, *Philos. Mag. B* **81**, 985 (2001).
- [8] M. Grünwald, P. Thomas, *Phys. Stat. Sol. (b)* **94**, 125 (1979).
- [9] D. Monroe, *Phys. Rev. Lett.* **54**, 146 (1985).
- [10] J. Noolandi, *Phys. Rev. B* **16**, 4474 (1977).
- [11] V. I. Arkhipov, A. I. Rudenko, *Phil. Mag. B* **45**, 189 (1982).
- [12] F.W. Schmidlin, *Phys Rev B* **16**, 2362 (1977).
- [13] V. I. Arkhipov, P. Heremans, E. V. Emelianova, G. J. Adriaenssens, *Appl. Phys. Lett.* **79**, 4154 (2001).
- [14] X. Jiang, Y. Harima, K. Yamashita, Y. Tada, J. Ohshita, A. Kunai, *Chem. Phys. Lett.* **364**, 616 (2002).
- [15] D. H. Dunlap, P. E. Parris, V. M. Kenkre, *Phys. Rev. Lett.* **77**, 542 (1996).
- [16] M. Pope, C. E. Swenberg, *Electronic Processes in Organic Crystals and Polymers*, 2nd edn. (University Press, Oxford, 1999).
- [17] V. I. Arkhipov, P. Heremans, E. V. Emelianova, G. J. Adriaenssens, H. Bässler, *Appl. Phys. Lett.* **82**, 3245 (2003).
- [18] C. Tanase, P. W. M. Blom, D. M. de Leeuw, E. J. Meijer, *Phys. Stat. Sol. (a)* **201**, 1236 (2004).
- [19] B. Maennig, M. Pfeiffer, A. Nollau, X. Zhou, K. Leo, P. Simon, *Phys. Rev. B* **64**, 195208 (2001).
- [20] L. Onsager, *J Chem. Phys.* **2**, 599 (1934).
- [21] L. Onsager, *Phys. Rev.* **54**, 554 (1938).
- [22] V. I. Arkhipov, P. Heremans, E. V. Emelianova, G. J. Adriaenssens, H. Bässler, *J. Phys.: Condensed Matter* **42**, 9899 (2002).
- [23] V. I. Arkhipov, E. V. Emelianova, G. J. Adriaenssens, *Phys. Rev. B* **64**, 125125 (2001).
- [24] M. A. Lampert, P. Mark, *Current Injection in Solids* (Academic Press, New York, 1970).
- [25] V. I. Arkhipov, E. V. Emelianova, Y. H. Tak, H. Bässler, *J. Appl. Phys.* **84**, 848 (1998).
- [26] T. Van Woudenberg, P. W. M. Blom, M. C. J. M. Vissenberg, J. N. Huilberts, *Appl. Phys. Lett.* **79**, 1697 (2001).
- [27] U. Wolf, V. I. Arkhipov, H. Bässler, *Phys. Rev. B* **59**, 7507 (1999).
- [28] V. I. Arkhipov, U. Wolf, H. Bässler, *Phys. Rev. B* **59**, 7514 (1999).
- [29] F. Schauer, R. Novotny, S. Nešpůrek, *J. Appl. Phys.* **81**, 1244 (1997).
- [30] P. M. Borsenberger, D. S. Weiss, *Organic Photoreceptors for Xerography* (Dekker, New York, 1998).
- [31] D. Emin, *Phys. Rev. B* **46**, 9419 (1992).
- [32] L. B. Schein, *Phil. Mag. B* **65**, 795 (1992).
- [33] P. E. Parris, V. M. Kenkre, D. H. Dunlap, *Phys. Rev. Lett.* **87**, 126601 (2001).
- [34] E. H. Magin, P. M. Borsenberger, *J. Appl. Phys.* **73**, 787 (1993).
- [35] H. Bässler, P. M. Borsenberger, R. J. Perry, *J. Polym. Sci. B: Polymer Phys.* **32**, 1677 (1994).
- [36] B. Hartenstein, H. Bässler, S. Heun, P. M. Borsenberger, M. Van der Auweraer, F. C. De Schryver, *Chem. Phys.* **191**, 321 (1995).
- [37] N. F. Mott, *J. Non-Cryst. Solids* **1**, 1 (1968).
- [38] S. D. Baranovskii, P. Thomas, G. J. Adriaenssens, *J. Non-Cryst. Solids* **190**, 283 (1995).
- [39] S. D. Baranovskii, T. Faber, F. Hensel, P. Thomas, *J. Phys. Condens. Matter* **9**, 2699 (1997).
- [40] M. Grünwald, B. Movaghar, B. Pohlmann, D. Würtz, *Phys. Rev. B* **32**, 8191 (1985).
- [41] V. I. Arkhipov, E. V. Emelianova, G. J. Adriaenssens, H. Bässler, *J. Non-Cryst. Solids* **299**, 1047 (2002).